

LEVEL II

12

AD A109388

THE ROLE OF ENVIRONMENT ON TIME DEPENDENT CRACK GROWTH

302 →  
JK R. E. Ricker and D. J. Duquette  
Rensselaer Polytechnic Institute  
Materials Engineering Department  
Troy, New York 12181

December 1981

(1) Technical Report to the Office of Naval Research

Contract No. N00014-67-A-0117-0012

No. N00014-75-C-0466, NR 036-093  
JK

Reproduction in whole or in part for any purpose of the U.S. Government is permitted. Distribution of this document is unlimited.

DTIC FILE COPY

P

DTIC  
ELECTE  
S JAN 7 1982 D  
D

82 01 07 011

# THE ROLE OF ENVIRONMENT ON TIME DEPENDENT CRACK GROWTH

R. E. Ricker and D. J. Duquette  
Materials Research Center  
Rensselaer Polytechnic Institute  
Troy, New York 12181

Gaseous as well as aqueous environments are known to accelerate time dependent crack growth under either static loading (SCC or HE) or dynamic loading conditions. In some cases, the rate controlling processes of these phenomena have been related to surface controlled reactions, while in other cases bulk reactions such as diffusion appear to be rate limiting. It is not entirely clear that the mechanisms of time dependent crack growth are identical for different environment/alloy couples, or for different ranges of loading conditions. This paper will attempt to examine the chemical aspects of environment/alloy interactions and to correlate those aspects with observed crack propagation rates under a variety of loading conditions at or near room temperature. Additionally, a brief discussion of the role of environment on elevated temperature fatigue crack growth will be presented.

Accession For	
NTIS GRA&I	<input checked="" type="checkbox"/>
DTIC TAB	<input type="checkbox"/>
Unannounced	<input type="checkbox"/>
Justification	
By	
Distribution/	
Availability Codes	
Dist	Avail and/or Special
A	

## Introduction

While it is generally accepted that aggressive environments accelerate crack propagation in cyclically loaded metals and alloys, the specific environmental reactions or chemico-mechanical processes which control the rates of crack propagation are not always understood.

The role of the environment is usually evaluated by conducting standardized tests under various controlled environmental conditions and comparing the results to those obtained in "neutral" environments (e.g. vacuum or inert gases) (1-4). The goal is to avoid failures by controlling or at least accurately predicting crack growth or initiation. The advent of fracture mechanics has led to the development of a semi-quantitative approach to these determinations. In this approach, the usable lifetime of a component is estimated by determining the time required for a pre-existing flaw to propagate to critical failure. The crack growth rate, and accordingly the service life, may be determined by the maximum possible rate of the environmental fracture mechanism, however, usually some slower environmental interaction, which must precede the actual fracture and is required by the fracture mechanism, is the rate determining step. Thus, changes in the crack propagation rate resulting from altering the aggressiveness of the environment may reflect the effect of these alterations on the rate determining step(s) and not on the actual fracture process.

## Mechanisms of Environmental Assisted Fracture

There are a large number of different fracture mechanisms which have been proposed to explain environmental assisted crack propagation. The details of each specific mechanism will not be discussed in this paper. However, the mechanisms which have been proposed are based on either:

1. Active corrosion of material at the crack tip
2. Adsorption of environmental species
3. Reactions in the bulk material ahead of the advancing crack
4. The formation of oxide films

Specific mechanisms differ in the process by which environmental factors combine with the strained metal to result in the actual fracture processes of crack extension. This combined effect occurs at the crack tip or in the plastic zone ahead of the crack tip. A series of events and/or reactions provide the required environmental influence to this fracture, and usually, these steps determine the rate of propagation and not the actual fracture process.

## Rate Limiting Steps

All of the proposed mechanisms require a sequence of generally discrete events or reactions for crack growth to occur. The rate determining step of a mechanism is, of course,



step if such a reaction occurs. The formation of oxide layers or the dissociation of environmental molecules would require such reaction steps (18,20).

Species in the local environment or liberated by chemical reactions may diffuse into a sample ahead of the advancing crack. In the highly strained region at the crack tip, the diffusing species may react with either the alloying elements of the sample or impurities in the sample. Also, if a supersaturation results in the plastic zone, the diffusing species may precipitate. Either the diffusion process or a chemical reaction step may be rate controlling. For example, these steps may be rate controlling for hydrogen embrittlement, internal oxidation, carburization, nitriding, or hydrogen attack (12,13). Diffusion can also be rate limiting for dealloying effects such as preferential oxidation, preferential dissolution (ie. dezincification), or evaporative losses of high vapor pressure alloy constituents (13).

The actual separation process could be the rate determining step, but no investigator has found this to be the case. Wei (5) estimated that for AISI 4340 steel the activation energy for the actual fracture process is less than 5 kJ/mole. This is considerably lower than the activation energies found for environmental assisted crack growth (5). The rate determining step in crack propagation is generally not the actual separation process, but usually some environmental interaction which is required for fracture.

#### Environmental Parameters

Several different environmental parameters are known to affect crack growth rates (14,15). These parameters include, but may not be limited to:

- I. Temperature
- II. Type of environment (bulk and local)
  - A. Gaseous
    - 1. Specific components
    - 2. Partial pressure
    - 3. Reactivity
  - B. Aqueous
    - 1. Solution species
    - 2. Solute concentration
    - 3. pH
    - 4. Electrode potential
    - 5. Solution viscosity
  - C. Others
    - 1. Liquid metals
    - 2. Organic solvents

Systematically altering any of these parameters or combinations of them may help to identify either the rate

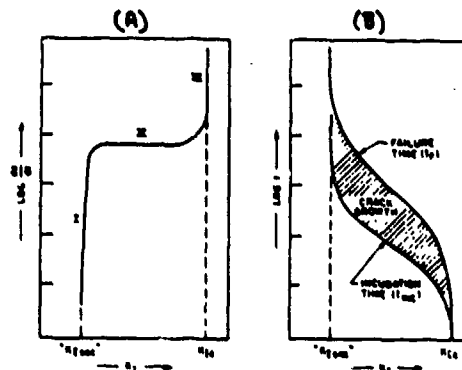
controlling step(s) or the environmental species responsible for crack propagation. Altering the temperature may allow the activation energy of crack propagation to be determined.

### Static Loading Crack Growth

Time dependent or sub-critical crack growth under static loading conditions is classified as either creep, stress corrosion cracking (SCC), liquid metal embrittlement (LME), or hydrogen embrittlement (HE). Delayed failure phenomena are influenced by the following parameters:

1. Applied stress or stress intensity factor
2. State of stress or loading mode
3. Metallurgical history
4. Crack geometry
5. Alloy composition
6. The environmental parameters listed above.

Figure 2: Schematic of crack growth rate (A) and time to failure curves (B) for static loading (14).



Tests are performed by placing either smooth samples or precracked samples into the environment and measuring either the time to failure or the actual crack propagation rates. The results of the tests are then plotted as shown in figure 2. Figure 2a shows a typical plot of crack propagation rate against the stress intensity factor for a precracked sample (15). From this it can be seen that there are three distinct stages of crack growth. In the first stage, the crack propagation rate increases rapidly with the stress intensity factor beginning at some stress intensity factor usually designated as the threshold stress intensity factor ( $K_{th}$  or  $K_{I SCC}$ ). In the second stage, crack growth is essentially independent of the stress intensity factor. In the final stage, crack propagation is again a strong function of the stress intensity as the crack approaches the critical flaw size (this stage is not always observed). In the first and third stages, crack propagation is strongly influenced by the stress intensity factor. In the second stage or the steady state stage, the crack propagation rate is generally believed to be determined by a rate limiting step.

Figure 3 shows the subcritical crack growth behavior of three different steels in hydrogen gas (14). In this figure,

two of the steels demonstrate stage 2 propagation which is independent of the mechanical driving force (as measured by the stress intensity factor). Since crack propagation is the result of combined mechanical and environmental factors, and since stage 2 propagation is independent of the magnitude of the mechanical contribution, then it is logical to assume that the rate of stage 2 growth is, in fact, determined by a rate controlling environmental reaction. By varying the temperature and measuring the rate of stage 2 propagation, the activation energy of crack propagation was evaluated (16). If this rate is determined by a single rate determining step, then the activation energy of crack propagation should be a measure of the activation energy of this reaction.

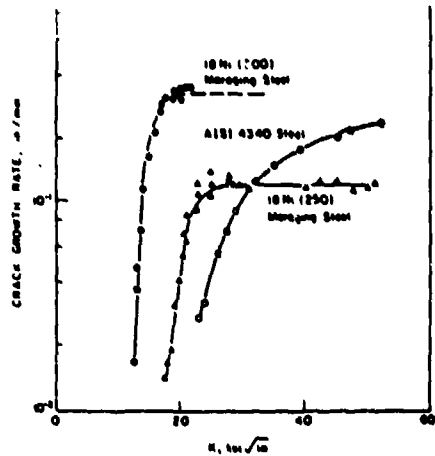


Figure 3: Influence of gaseous hydrogen (1 atm.) on the static loading crack growth rate of three steels (14).

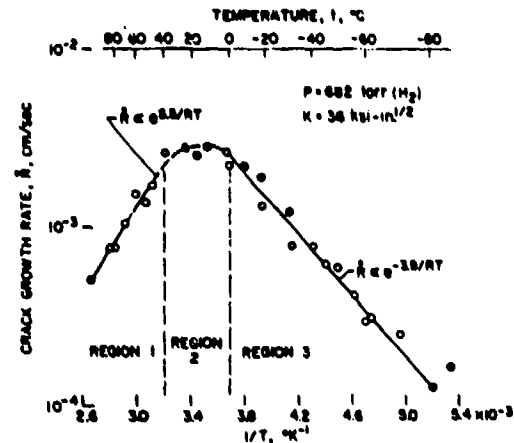


Figure 4: Arrhenius plot of the static temperature dependence of the static loading steady state Crack growth rate for AISI 4130 steel in gaseous hydrogen (17).

Figure 4 is a plot of the reciprocal of temperature against the rate of crack growth for a AISI 4130 steel in hydrogen gas (17). In this figure, three different regions of behavior are shown. At low temperatures (<0°C) the mean stage 2 growth rate increases with increasing temperature (region 3 in figure 4). At higher temperatures (>40°C), the crack growth rate decreases with increasing temperature (region 1 in figure 4). Between these two regions is a transition region where crack growth is almost independent of temperature (region 2 in figure 4). Both regions 1 and 3 show Arrhenius type temperature dependence with activation energies of -23 and +18 kJ/mole respectively (17,20).

Figure 5 shows the pressure dependence of the crack growth rate at constant stress intensity in each of the three regions of temperature behavior discussed above. A different pressure dependence was found for each of the three regions. At low temperatures (region 3), the crack growth rate varied with the square root of the hydrogen gas pressure. At high temperatures (region 1), the crack growth rate varied directly with the pressure. At intermediate temperatures, region 2, the growth rate varied with the hydrogen gas pressure to the 1.5 power. Since the activation energy for hydrogen permeation (36 kJ/mole) is very different from the activation energy measured for crack propagation (18 kJ/mole), this is not the rate controlling step

of hydrogen embrittlement under these conditions. Williams and Nelson (17) recognized that the shape of the crack growth rate vs. reciprocal temperature curve, figure 4, is of the same basic shape as an adsorption rate vs. reciprocal temperature curve for thermally activated adsorption. Accordingly, they developed a model for the crack growth rate using the hydrogen adsorption results of Porter and Tompkins (38). This model explains both the temperature dependence of figure 4 and the pressure dependence of figure 5. According to this model, the activation energy of the low temperature region, region 3, is the energy of migration from the "initial" adsorption sites. Also, according to this model, the activation energy measured for the high temperature region, region 1 in figure 4, is the sum of the heat of adsorption and the energy of migration. The activation energies found in figure 4 are in the range of values found by Porter and Tompkins (38). Williams and Nelson concluded that the crack growth rate in this environment is controlled by a heterogeneous reaction involving the transition of hydrogen from its molecular form in the gas phase to its atomic form on the crack surface (21). To circumvent this slow step, Nelson et. al. tested samples in a partially dissociated hydrogen gas environment (21). They found, as shown in figure 6, that the three distinct regions of thermally activated crack growth no longer existed, that the activation energy for propagation changed, and that the rate of crack propagation was greatly accelerated as compared to that observed for the same pressure of molecular hydrogen gas (17). They determined the apparent activation energy for this environment to be +28.5 kJ/mole (21). Comparing this to the activation energies of permeation, +35.6 kJ/mole, lattice diffusion, +7.9 kJ/mole, and the apparent heat of solution, +27.2 kJ/mole, they concluded that the rate controlling reaction was the establishment of a hydrogen population in the ferrous lattice just below the crack tip surface (21). The morphology of the fracture surfaces in this environment was virtually unchanged from that observed in the molecular hydrogen gas environment. These investigators concluded that the specific mechanism of hydrogen induced cracking did not change as a function of molecular or atomic hydrogen atmosphere but that only the rate determining step changed (21).

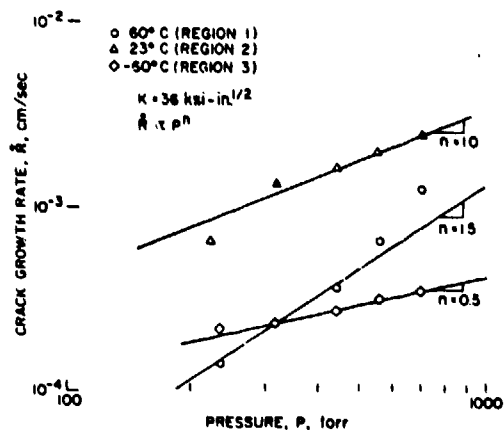


Figure 5: The effect of hydrogen gas pressure on the static loading steady state crack growth rate of AISI 4130 steel (17).

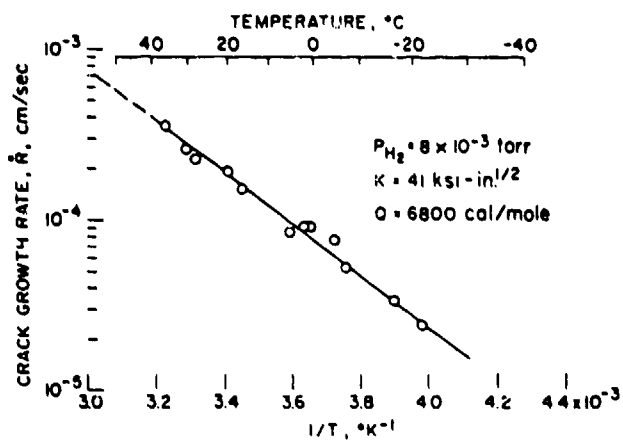


Figure 6: Arrhenius plot of the temperature dependence of static loading steady state crack growth rate in a dissociated hydrogen gas environment (21).

A change of environment from a gas to an aqueous solution adds significantly to the complexity of the problem. In addition to the effects of solute type and concentration in the solution, there is also the possibility of reactions with the water itself to produce hydrogen gas, oxide films, and/or pH changes in the growing cracks.

Van Der Sluys studied the effect of varying electrochemical potential and pH on the crack growth rate of cracks in an AISI 4340 steel (22). Figure 7 shows the potential vs. crack growth rate in three different pH solutions. The curves show basically three different regions of potential vs. growth rate behavior. First, at potentials active compared to the hydrogen evolution potential, the growth rate increases with decreasing potential and accordingly increasing hydrogen fugacity. Second, a plateau is observed in the region of water stability (above the potential for cathodic hydrogen evolution and below the potential where oxygen evolution begins) and third, the growth rate decreases with increasing potentials above the oxygen evolution potential (22). The drop off at passive potentials was not very great. In the pH 2 solution, the growth rate actually increased with potentials above the oxygen evolution potential (figure 7). Van Der Sluys (22) concluded that at cathodic potentials hydrogen embrittlement is the dominant mechanism of crack growth and at anodic potentials dissolution is the dominant mechanism of crack growth.

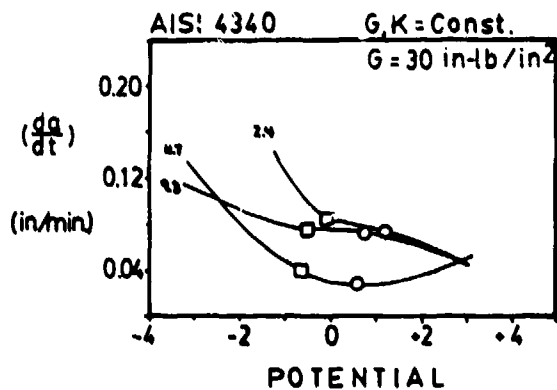


Figure 7: Crack growth rate under static loading at constant stress intensity vs. electrochemical potential in solutions of pH=2.4, 9.3 and 11.7 (22).  
°=oxygen evolution potential  
■=hydrogen evolution potential

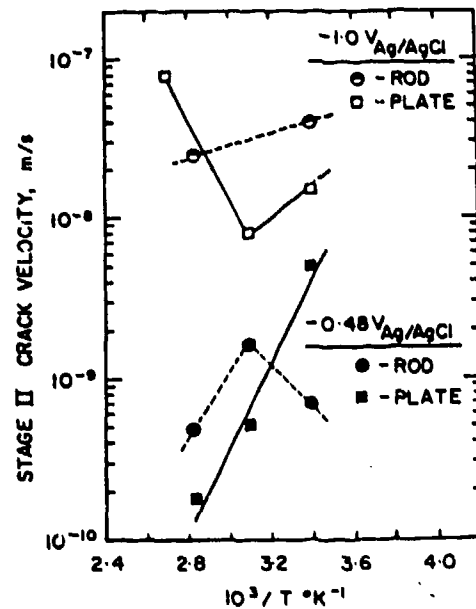


Figure 8: Arrhenius plot of the temperature dependence of the static loading steady state crack growth rate of HY-180M steel in 3.5% sodium chloride at two electrochemical potentials (23).

Bala and Tromans studied the crack growth rate of HY-180M steel in a 3.5% NaCl solution (23,24). They found a strong dependence of crack growth rate on potential. No crack growth

occurred at  $-0.52$  V(SHE) but, crack growth did occur at potentials both above and below this value (The reversible potential for iron in this solution is  $-0.53$  V(SHE)) (23,24). They also concluded that hydrogen embrittlement was responsible for cracking at active potentials while anodic dissolution was involved at noble potentials. However, while studying the effects of temperature on the crack growth rate, these authors observed the same effect of increasing temperature in promoting more transgranular SCC at a cathodic potential ( $-1.0$  V Ag/AgCl) and at an anodic potential ( $-0.48$  V Ag/AgCl). As a result, they altered their earlier conclusion and concluded that the same mechanism, hydrogen embrittlement, was responsible for fracture in both potential ranges (24). The activation energy of a rate determining process could not be determined from an Arrhenius type analysis as shown in figure 8. This result indicates that crack growth, which is much slower than that shown for the AISI 4130 steel shown in figure 4, is under mixed rate control. Processes which may contribute to the control of the growth rate are hydrogen ion discharge, surface adsorption and migration, and lattice transport of atomic hydrogen. At anodic potentials, the kinetics of anodic dissolution and subsequent hydrolysis reactions, which lower the pH, thus making hydrogen evolution possible, may further limit the crack growth rate (Figure 8) (24).

#### Cyclic Loading Crack Growth

Crack growth processes under cyclic loading conditions are more complex than for static loading conditions. In addition to the parameters discussed above, crack growth under cyclic loading is influenced by the following variables:

1. Peak Stress Intensity ( $K(\max)$ )
2. Stress Intensity Range ( $\Delta K$ )
3. Stress Ratio ( $R$ )
4. Frequency ( $f$ )
5. Load Waveform

Figure 9 shows three different types of crack propagation curves typical of corrosion fatigue (15). Type A is typical of a material in an aggressive environment where stress corrosion cracking does not occur. The environment reduces the threshold stress intensity factor for the initiation of crack propagation. Also, the relative influence of the environment on the crack growth rate is reduced as the rate of crack growth increases. This is typical of materials such as aluminum in pure water (15,25).

The second type of propagation shown in figure 9, type B, is for an environment which causes stress corrosion cracking. At stresses below the stress corrosion threshold, the environment has no effect on crack propagation. However, as the maximum stress intensity in the load cycle increases, it eventually reaches and exceeds the stress corrosion threshold. When this occurs the crack growth rate increases sharply. This type of propagation is observed in steels in aqueous

environments (18-20). The third type, type C, is more representative of what is commonly observed in service; a combination of the two previous types.

Air is, of course, the most commonly encountered gaseous environment and has a significant effect on the fatigue properties of most engineering alloys. Usually, fatigue crack propagation in air is increased with respect to vacuum at the same temperature. Oxygen and water vapor are usually responsible for this detrimental effect. However, under certain conditions, exposure to air can retard or even arrest crack propagation (29-31).

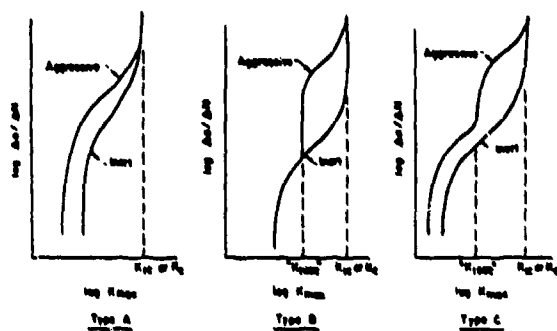


Figure 9: Three basic types of corrosion fatigue crack growth behavior (27).

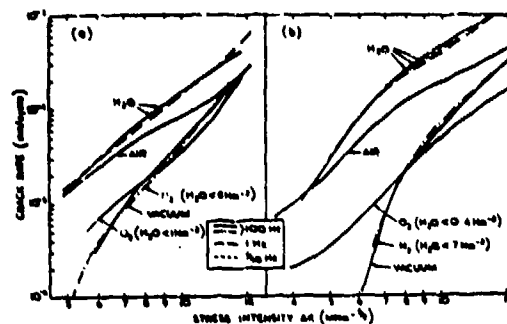


Figure 10: Fatigue crack growth of two aluminum alloys in various environments and vacuum at a loading frequency of 100 Hz (26).

(a). Al-2.5Cu-1.5Mg-1.2Ni  
(b). Al-5.8Zn-2.7Mg-1.3Cu

Figure 10 shows the effects of gaseous environments on fatigue crack propagation of two aluminum alloys (26). Water vapor is the most detrimental component in the gaseous atmosphere for these alloys. However, for nickel alloys, oxygen is the most detrimental species, and for high strength steels both water vapor and oxygen are equally detrimental.

The effect of gas pressures on crack propagation usually follows a step or "S" type behavior with some critical pressure range separating a plateau of no effect from a plateau where saturation of the effect occurs. This type of behavior is shown in Figure 11 (27) where the crack growth rate for three stress intensity ranges are plotted against the partial pressure of water vapor for aluminum alloy 2219-T851 (27,25). At pressures below the critical pressure, the crack growth rate rapidly approaches that observed in vacuum or in argon gas. Pao et. al. (39) found that, for an AISI 4340 steel in water vapor, the frequency where the minimum in crack growth rate was reached corresponded to the point where the exposure per cycle (pressure/2xfrequency) was not great enough for the onset of oxidation. Also, they found that the maximum crack growth rate per cycle corresponded to the exposure per cycle where the oxidation of the steel surface at the crack tip was essentially complete (39). However, Wei et. al. (25,27) found that this approach required an adjustment of three orders of magnitude to fit the data of figure 11. As a result, they assumed that the rate of mass transport must be the crack growth rate limiting

step. The limited transport of water vapor to the crack tip and the rapid reaction rate of aluminum and water vapor results in an effectively reduced gas pressure at the crack tip. Therefore, the exposure of the metal at the crack tip to the damaging environment for an aluminum alloy is less than that assumed by the model of Pao et. al. (39). By using reaction rate data and assuming Knudsen flow up the crack, Wei et. al. (27) estimated that an essentially constant reduced pressure develops at the crack tip and then used this pressure in the previous model to derive the line shown in figure 12 (27,25).

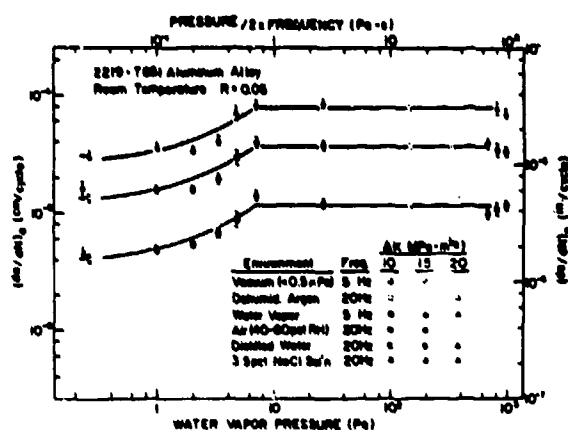


Figure 11: Influence of water vapor pressure on fatigue crack growth rate in 2219-T851 aluminum alloy (25).

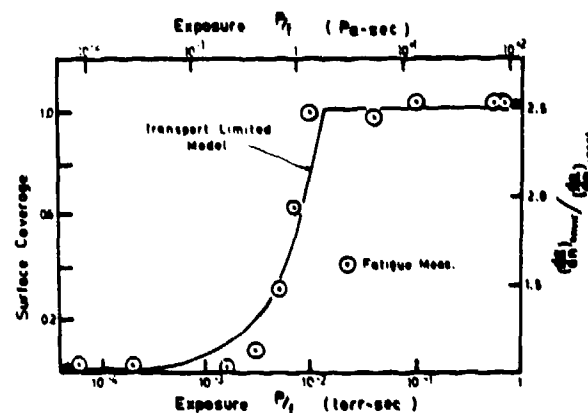


Figure 12: Comparison of the observed fatigue crack growth response for 2219-T851 aluminum alloy in water vapor and a transport-limited rate model (25).

Environment also has significant effects at elevated temperatures. For example, figure 13 shows the effect of oxygen pressure on the crack growth rate of 316 stainless steel at 500°C (28). The same type of critical pressure effect is observed at this temperature as is typically found at lower temperatures. The fatigue lives of a nickel base superalloy (MAR-M200) at three different temperatures in air and vacuum are shown in figure 14 (1,2,29). From this it can be seen that at two temperatures, air accelerated failure, while at 760°C (1400°F) air has no effect and at 925°C (1700°F) air retards failure. Austin (31) found that at room temperature a directionally solidified Cobalt-base eutectic (COTAC) demonstrated accelerated crack propagation and a reduced threshold in air as compared to vacuum (figure 15a). At elevated temperatures, crack propagation in vacuum increased compared to room temperature vacuum tests (figure 15b). However, at temperatures above approximately 600°C crack propagation did not occur in air for the medium and low stress intensities shown in figure 15. Introduction of air into the vacuum chamber of a propagating fatigue crack at 750°C resulted in immediate arrest and increasing the stress range resulted in propagation followed by another arrest (31). Alternating stress intensity levels which resulted in continued propagation caused failure in less than a thousand cycles (31). It was concluded that, the positive volume change of oxidation at the crack tip results in reducing the effective alternating stress intensity and increasing the mean stress intensity (31).

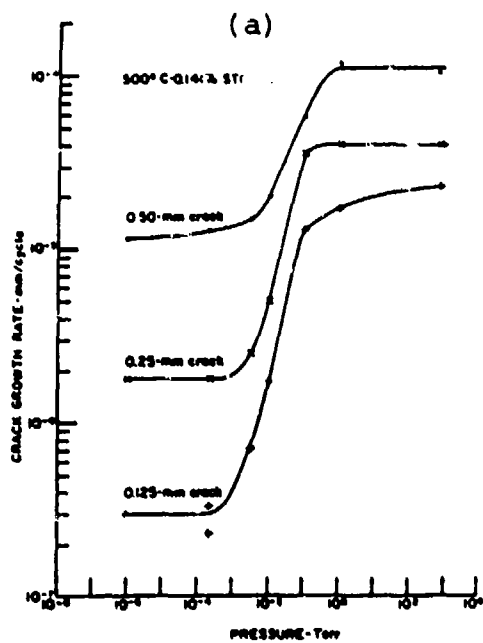


Figure 13: Effect of oxygen pressure on fatigue crack growth rate of type 316 stainless steel at 500°C (28).

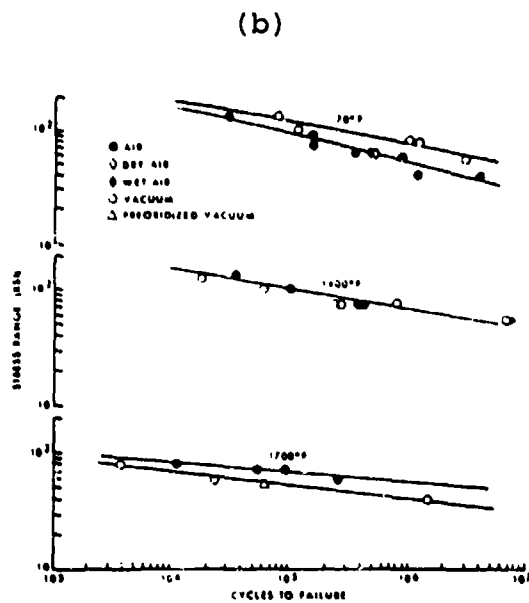


Figure 14: Fatigue life of nickel superalloy single crystals (low carbon MAR-M200) in air and vacuum at 20, 760 and 925°C (1).

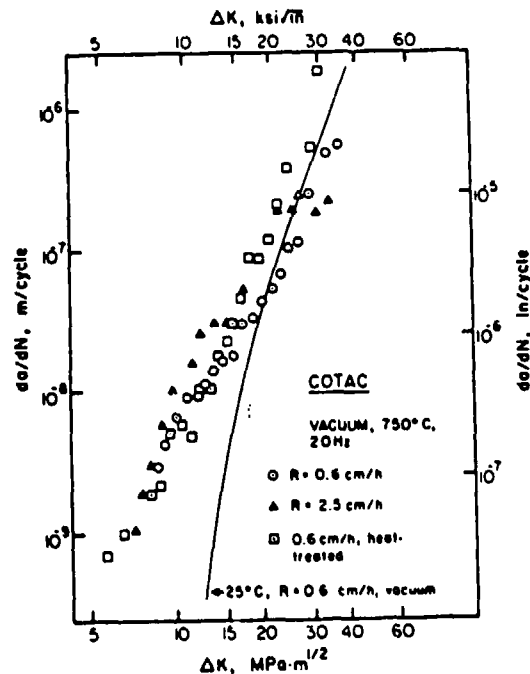
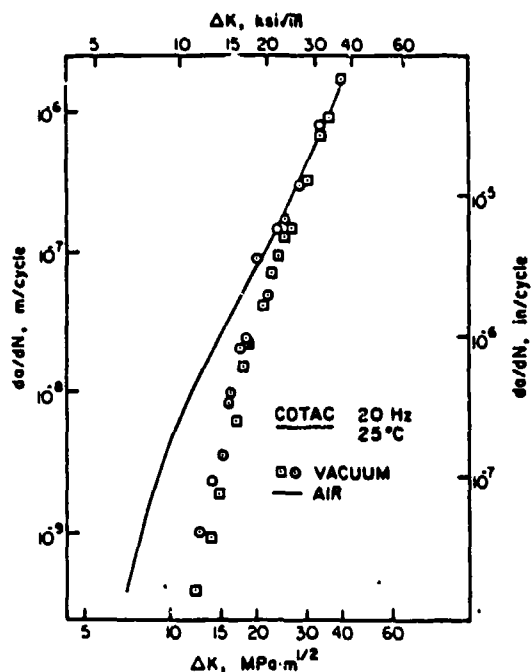


Figure 15: Fatigue crack growth in a cobalt base directionally solidified eutectic in air and vacuum at 25°C (a) and 750°C (b) (31).

Aqueous solutions are generally aggressive and, as with static loading, aqueous solutions are more difficult to analyze than are single component gaseous environments. The effect of frequency and waveform in aqueous solutions have been studied by

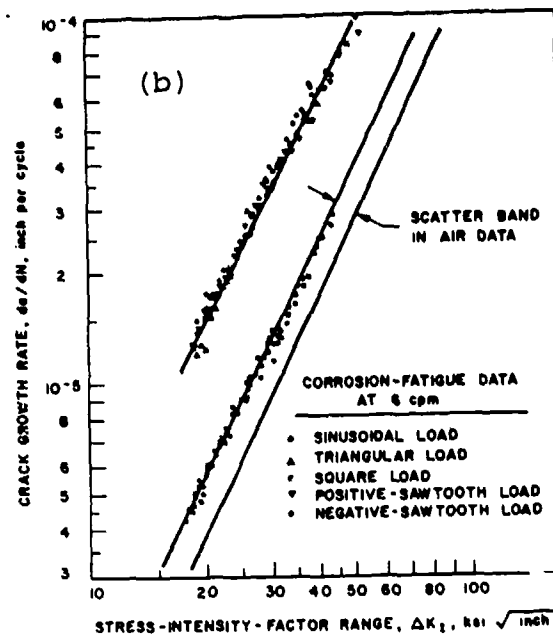
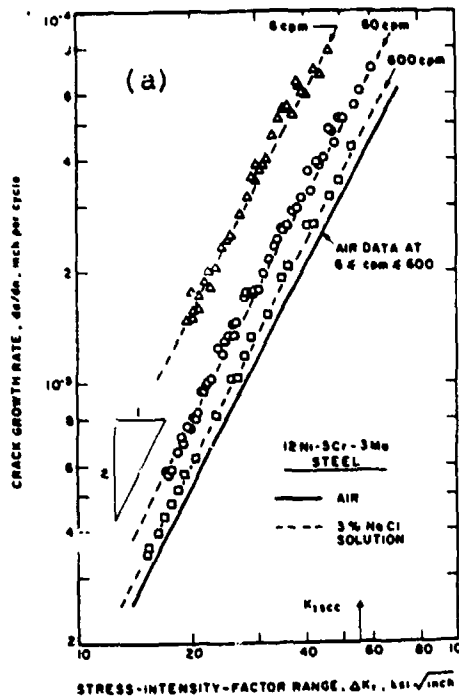


Figure 16: Effect of loading variables on the corrosion fatigue crack growth of a 12Ni-5Cr-3Mo steel in 3.0% sodium chloride solution: (a) Frequency effect and (b) Load waveform effect (32).

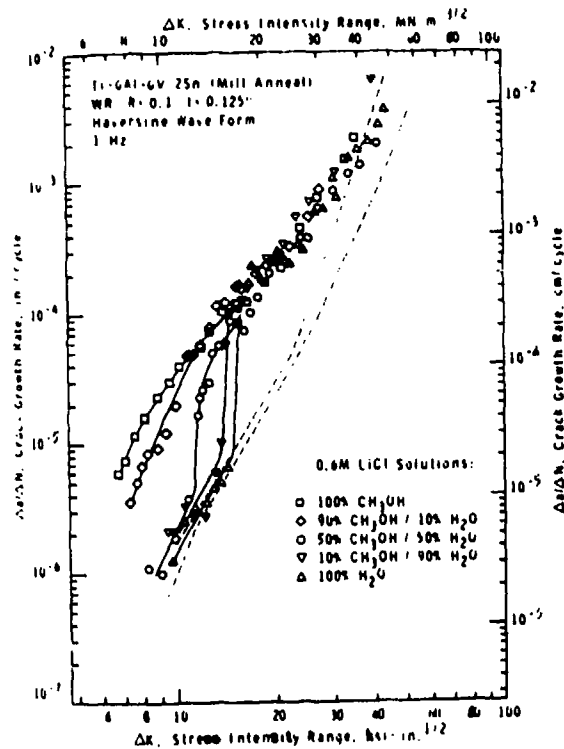
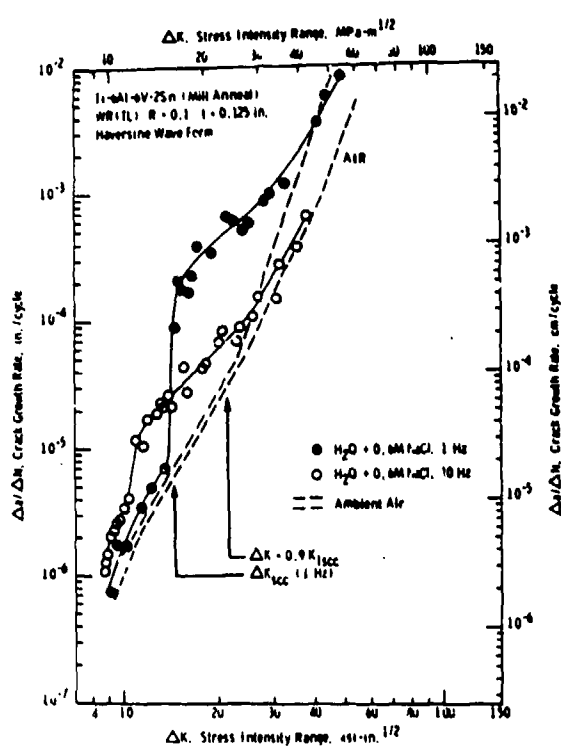


Figure 17: Effect of loading frequency on the fatigue crack growth rate of a 6Al-6V-2Sn titanium alloy in 0.6N sodium chloride solution (35).

Figure 18: Effect of water additions on the fatigue crack titanium alloy in a 0.6 N lithium chloride methanol Solution (36).

many different investigators. For example, Barsom (32,33) studied the effects of these variables on steels below the stress corrosion cracking threshold. Figure 16a (32) shows the effect of frequency on the crack growth rate. Barsom found that the propagation followed the Paris-Erdogan (34) equation at all frequencies:  $da/dN = D(t)(\Delta K)^2$ . Only the pre-exponential coefficient  $D(t)$  varied with the environment and frequency. In air,  $D(t)$  was a constant, independent of frequency. In sodium chloride solution,  $D(t)$  increased with decreasing frequency (figure 16a). By changing the waveform at a constant frequency (6 Hz), it was found (Figure 16b), that the rising portion of the load wave form was responsible for the environmental damage observed (Figure 16b). Sinusoidal, triangular, and positive sawtooth waves all had the same crack growth rates. However, fast rise time square waves and negative sawtooth forms had the same crack growth rate in the 3% sodium chloride solution as all of the waveforms had in air.

Figure 17 shows the behavior of a Ti-6% Al-6% V-2% Sn alloy in an aqueous environment which causes stress corrosion cracking (0.6M NaCl) (35). This shows the typical crack propagation behavior for this type of corrosion fatigue system as shown above in figure 9. However, the stress intensity range where stress corrosion cracking apparently begins is below that where the peak stress intensity ( $K_{max}$ ) is equal to the statically measured threshold. Above this apparent stress corrosion cracking level, decreasing the frequency increased the crack propagation rate. Below this level, the opposite frequency effect was found. The level of the transition, the stress intensity range for stress corrosion cracking, increased with decreasing frequency approaching the statically measured value. Methanol causes intergranular corrosion of this alloy and, if a load is applied, intergranular cracking. Figure 18 shows the effect of combining two corrosive environments in different ratios (36). Apparently repassivation of the surface cannot occur in pure methanol and adding water allows passivation to occur below the level for stress corrosion cracking. Above the stress corrosion cracking threshold, the crack propagation rate is greater than the beneficial repassivation rate. This explains the shift in the observed stress intensity range for stress corrosion cracking with frequency and the cross over in frequency effect. That is, above the apparent stress corrosion threshold, slower frequencies allow more dissolution and hydrogen evolution per cycle resulting in more crack growth per cycle. However, below the critical level, slower frequencies allow a thicker protective layer to form resulting in less crack growth per cycle. Since passivation occurs at a relatively fixed rate, the critical stress intensity range where passivation of the metal at the crack tip stops, decreases with increasing frequency (36).

#### DISCUSSION

The crack growth rate curves of sub-critical crack propagation under static loading conditions exhibit three characteristic features (fig. 2). These three features are the threshold stress intensity factor, the steady state or stage 2 crack growth rate and the stress intensity of final critical fracture which is a materials constant. Both the steady state or stage 2 crack growth rate and the stress intensity threshold

for crack growth are characteristic of the environment and the mechanical loading conditions.

The crack growth rate plateau in stage 2 is believed to result from a rate limiting environmental reaction or step. This is a critical assumption which makes this feature important for analyzing the role of the environment in time dependent crack propagation. The assumption that the steady state crack growth rate is determined by a rate determining environmental step is based upon two observations. First, environmental assisted crack propagation is the result of the combination of mechanical and environmental factors and second, the crack growth rate appears to be independent of the mechanical contribution. By varying environmental factors and measuring the steady state crack growth rate, the rate determining environmental reaction(s) or step(s) can be studied. However, by studying both the environmental reactions and the crack growth rate, something can be learned about the fundamental environmental fracture process other than the identification of undesirable environmental conditions or species.

The threshold stress intensity factor has not been discussed in detail in the preceding sections. While it is an important parameter, this paper has concentrated on crack propagation and not on the initiation stage of crack growth. In this stage, there is more than sufficient environmental contribution for fracture but barely enough mechanical driving force. That is, the threshold stress intensity for crack propagation is the minimum required mechanical contribution to the fracture process for fixed equilibrium or steady state environmental conditions.

Three regions are also found in the crack growth curves for dynamic loading. However, these three regions are present in both inert and aggressive environments. There is no feature, such as the steady state crack growth rate, which can be attributed solely to the environmental component of crack growth and then used to identify the rate determining environmental processes. However, the superposition model of Wei and Landes (37) can be used to attempt to separate the relative contributions of environmental effects from purely mechanical fatigue damage (15,27). This model assumes that these two effects are independent of each other or that they can be analyzed as such. According to this assumption, the environmental contribution to crack growth can be found by subtracting the crack growth rate measured in an inert reference environment (R) from that measured in the aggressive environment (E). Mathematically this is expressed as:

$$\left(\frac{da}{dN}\right)_E - \left(\frac{da}{dN}\right)_R = \left(\frac{da}{dN}\right)_{\Delta E}$$

This equation yields a crack propagation rate increase due to the aggressive environment vs. alternating stress intensity curve. This environmental contribution to the fatigue crack growth rate can be analyzed to determine the origin(s) of the environmental effects. The environmental term may be a single effect or it may result from the summation of different effects. Different environmental assisted fracture mechanisms may be competing. Distinction between effects can be made by varying

environmental variables and loading variables such as temperature, pressure, loading frequency and loading waveform.

Wei and Landes (37) originally identified a sustained load or stress corrosion component to crack growth for loads during the load cycle above the stress corrosion cracking threshold. This term is calculated from the static loading loading crack growth data obtained in an identical environment. This stress corrosion term is sufficient for modeling the corrosion fatigue behavior of various steels and titanium but not for the aluminum/water system where there is a strong interaction of the corrosive environment and the cyclic loading. This stress corrosion term is sufficient for systems which demonstrate the type of corrosion fatigue illustrated by type B in figure 9. Additional environmental interaction terms are required to model the more general types of corrosion fatigue illustrated in figure 9. Weir et. al. (30) and Wei and Simmons (40) have examined the interaction of corrosive environments and cyclic loading. These investigators have developed surface reaction control and transport control terms. More recently, Wei and Shim (41) have extended these terms to represent frequency and temperature effects in aqueous solutions.

The object of this discussion is not to describe these models in detail, but to demonstrate that reasonable models for corrosion fatigue crack growth, and in the future static environmental assisted crack growth, are being developed. Also, to show that, as has frequently been pointed out by Wei and co-workers, environmental crack propagation tests alone will not answer all of the questions about the role of the environment in time dependent crack growth unless they are supplemented with quantitative chemical and metallurgical examinations. That is, a totally integrated approach will be required to reach a complete understanding of this problem.

#### Summary

This paper has shown that gaseous as well as aqueous environments will accelerate time dependent crack growth under both static and dynamic loading conditions. Also, to illustrate the complexity of this problem, examples have been shown where an aggressive environment (air at elevated temperatures) will actually delay failure or arrest crack growth. Crack growth behavior depends strongly on the exact nature of the environment, the samples reactivity in this specific environment, and loading and metallurgical variables. Complete understanding of the role of the environment in time dependent crack growth can only follow from thorough integrated investigations into all of these factors.

#### Acknowledgment

The authors would like to acknowledge the support of the U.S. Office of Naval Research under Contract #N00014-75-C-0466.

## References

1. M. Gell & D. J. Duquette, "The Effects of Oxygen on Fatigue Fracture of Engineering Alloys", Corrosion Fatigue, NACE-2 (1972) p366.
2. D. J. Duquette & M. Gell, "The Effects of Environment on the Elevated Temperature Fatigue Behavior of Nickel-Base Superalloy Single Crystals", Met Trans, V3, July 1972, p1899.
3. H. N. Hahn, "Corrosion Fatigue Behavior of Copper and Copper Base Alloys", PhD Thesis, Rensselaer Polytechnic Institute, Troy, NY, May 1977.
4. T. W. Crooker, "The Need for Standards Development in Corrosion Fatigue Testing with Precracked Specimens", ASTM Standardization News, May 1975, p17.
5. R. P. Wei, "Rate Controlling Processes and Crack Growth Response", Hydrogen Effects in Metals, Ed. A. W. Thompson & I. M. Bernstein, TMS-AIME, Warrendale, PA, (1981) p677.
6. S. P. Lynch, "Mechanisms of Fatigue and Environmentally Assisted Fatigue", Fatigue Mechanisms, J. T. Fong ed., ASTM-STP-675, Kansas City, May (1978) p 174.
7. S. P. Lynch, "A Comparative Study of Stress-Corrosion Cracking, Hydrogen-Assisted Cracking and Liquid-Metal Embrittlement" Hydrogen Effects in Metals, *ibid* p863.
8. F. P. Ford, "Corrosion Fatigue Crack Propagation in Al- 7% Mg Alloy", Corrosion, V35, #7 (1979) p281.
9. F. P. Ford, "Quantitative Examination of Slip-Dissolution and Hydrogen-Embrittlement Theories of Cracking in Al alloys", Met Sci, July 1978, p326.
10. J. A. Feeney, J. C. McMillan, R. P. Wei, "Environmental Fatigue Crack Propagation of Al Alloys at Low Stress Intensity Levels", Met Trans, V1 (1970) p1741.
11. R. P. Wei, "Fatigue-Crack Propagation in a High-Strength Aluminum Alloy", Intl J of Fracture, V4, #2 (1968) p159.
12. A. S. Tetelman, "Recent Developments In Classical (Internal) Hydrogen Embrittlement", Hydrogen in Metals, Ed. I. M. Bernstein & A. W. Thompson, American Society for Metals, Metals Park, OH, (1974) p.17.
13. R. H. Cook & R. P. Skelton, "Environment-Dependence of the Mechanical Properties of Metals at High Temperatures", Intl Metl Rev, V19 (1974) p199.
14. R. P. Wei, "The Effect of Temperature and Environment on Subcritical-Crack Growth", Fracture Prevention and Control, Ed. D. W. Hoepfner, ASM Metals Park, Ohio (1974) p73.
15. R. P. Wei, "On Understanding Environment Enhanced Fatigue Crack Growth A Perspective View (1963-1977)", Tech Rpt #7, ONR Cont N00014-75-C-0543, NR 036-097, May 1978.

16. H. Eyring & E. M. Eyring, Modern Chemical Kinetics, Reinhold Publ. Corp. NY (1963).
17. D. P. Williams & H. G. Nelson, "Embrittlement of 4130 Steel by Low Pressure Gaseous Hydrogen", Met Trans, V1, #1 (1970) p63.
18. G. W. Simmons, P. S. Pao, R. P. Wei, "Fracture Mechanics and Surface Chemistry Studies of Subcritical Crack Growth in AISI 4340 Steel", Met Trans A, V9A, August 1978, p1147.
19. R. P. Gangloff & R. P. Wei, "Gaseous Hydrogen Embrittlement of High Strength Steels", Met Trans A, V8A, July 1977, p1043.
20. G. W. Simmons, P. S. Pao, R. P. Wei, "Fracture Mechanics and Surface Chemistry Studies of Subcritical Crack Growth in AISI 4340 Steel", Tech. Rpt #4, ONR Cont N00014-15-C-0543, NRC36-097, September 1977.
21. H. G. Nelson, D. P. Williams, A. S. Tetelman, "Embrittlement of a Ferrous Alloy in a Partially Dissociated Hydrogen Environment", Met Trans, V2, April 1971, p953.
22. W. A. Van Der Sluys, "Mechanisms of Environment Induced subcritical Flow Growth in AISI 4340 Steel", Engr Frac Mech, V1 (1969) p447.
23. S. R. Bala & D. Tromans, "Effect of Temperature Upon Stress Corrosion Cracking of HY-180M Steel in 3.5 Pct NaCl", Met Trans A, V11A, July 1980, p1161.
24. S. R. Bala & D. Tromans, "Stress Corrosion Cracking of High Strength HY-180M Steel in 3.5 Pct NaCl", Met Trans A, V9A (1978) p1125.
25. R. P. Wei, P. S. Pao, R. G. Hart, T. W. Weir, G. W. Simmons, "Fracture Mechanics & Surface Chemistry Studies of Fatigue Crack Growth in an Al Alloy", Met Trans A, January 1980, V11A, p151.
26. F. J. Bradshaw & C. Wheeler, "The Influence of Gaseous Environments and Fatigue Cracks in Some Al Alloys", Intl J of Fract Mech, V5, #4, December 1969, p255.
27. R. P. Wei & G. W. Simmons, "Recent Progress in Understanding Environment Assisted Fatigue Crack Growth", Tech. Rpt #8, ONR N00014-75-C-0543, NR 036-097, January 1979.
28. H. H. Smith, P. Shahinian, M. R. Achter, "Fatigue Crack Growth Rates in Type 316 Stainless Steel at Elevated Temperature as a Function of Oxygen Pressure", Trans TMS-AIME, V245, May 1969, p947.
29. D. J. Duquette & M. Gell, "The Effect of Environment on the Mechanism of Stage I Fatigue Fracture", Met Trans, V2, May 1971, p1325.
30. T. W. Weir, R. G. Hart, G. W. Simmons, & R. P. Wei, "A Model for Surface Reaction and Transport Controlled Fatigue Crack Growth", Scripta Met., Vol. 14, (1980), p. 357.
31. C. M. Austin, "Fatigue Crack Propagation in a Directionally

Solidified Cobalt-Base Eutectic", PhD thesis, Rensselaer Polytechnic Institute, Troy, NY, December 1979.

32. J. M. Barsom, "Effect of Cyclic Stress Form on Corrosion Fatigue Crack Propagation Below  $K(I_{SCC})$  in a High Yield Strength Steel", Corrosion Fatigue, NACE-2 (1972) p424.

33. J. M. Barsom, "Corrosion-Fatigue Crack Propagation Below  $K(I_{SCC})$ ", Engr Fract Mech, V3 (1971) p15.

34. P. C. Paris & F. Erdogan, "A Critical Analysis of Crack Propagation Laws", J Basic Engr, V85 (1963) p528.

35. D. B. Dawson & R. M. N. Pelloux, "Corrosion Fatigue Crack Growth of Titanium Alloys in Aqueous Environments", Met Trans, V5, March 1974, p723.

36. D. B. Dawson, "Fatigue Crack Growth Behavior of Ti-6Al-6V-2Sn Methanol and Methanol-Water Solutions", Met Trans A, V12A, May 1981, p791.

37. R. P. Wei & J. D. Landes, "Correlation Between Sustained-Load and Fatigue Crack Growth in High-Strength Steels", Matls Res and Stds, ASTM, July 1969, p25.

38. A. S. Porter and F. C. Tompkins, "The Sorption of Hydrogen and Other Gases by Evaporated Iron Films", Proc. Roy. Soc. London, V A217, (1953), p. 544.

39. P. S. Pao, W. Wei, R. P. Wei, "Effect of Frequency on Fatigue Crack Growth Response of AISI 4340 Steel in Water Vapor", Environmental Sensitive Fracture on Engineering Materials, Z. A. Foroulis ed. TMS-AIME, Warrendale, PA., (1979), p. 565.

40. R. P. Wei and G. W. Simmons, "Surface Reactions and Fatigue Crack Growth", Proceedings, 27th Army Materials Research Conf., Bolton Landing, NY, July 1980, (to be published).

41. R. P. Wei and G. Shim, "Fracture Mechanics and Corrosion Fatigue" Proceedings, ASTM Corrosion Fatigue Conf., St. Louis Mo., Oct. 1981, (to be published).

**Security Classification**

**DOCUMENT CONTROL DATA - R&D**

*(Security classification of title, body of abstract and indexing annotation must be entered when the overall report is classified)*

<b>1. ORIGINATING ACTIVITY (Corporate author)</b> Rensselaer Polytechnic Institute Materials Engineering Department Troy, New York 12181		<b>2a. REPORT SECURITY CLASSIFICATION</b> Unclassified	
		<b>2b. GROUP</b>	
<b>3. REPORT TITLE</b> THE ROLE OF ENVIRONMENT ON TIME DEPENDENT CRACK GROWTH			
<b>4. DESCRIPTIVE NOTES (Type of report and inclusive dates)</b> Technical Report			
<b>5. AUTHOR(S) (Last name, first name, initial)</b> Ricker, R. E. Duquette, D. J.			
<b>6. REPORT DATE</b> December, 1981		<b>7a. TOTAL NO. OF PAGES</b> 19	<b>7b. NO. OF REFS</b> 41
<b>8a. CONTRACT OR GRANT NO.</b> #N00014-75-C-0466, NRO36-093		<b>8a. ORIGINATOR'S REPORT NUMBER(S)</b>	
<b>a. PROJECT NO.</b>			
<b>c.</b>		<b>8b. OTHER REPORT NO(S) (Any other numbers that may be assigned this report)</b>	
<b>d.</b>			
<b>10. AVAILABILITY/LIMITATION NOTICES</b> Distribution of this document is unlimited.			
<b>11. SUPPLEMENTARY NOTES</b>		<b>12. SPONSORING MILITARY ACTIVITY</b> OFFICE OF NAVAL RESEARCH	
<b>13. ABSTRACT</b> Gaseous as well as aqueous environments are known to accelerate time dependent crack growth under either static loading (SCC or HE) or dynamic loading conditions. In some cases, the rate controlling processes of these phenomena have been related to surface controlled reactions, while in other cases bulk reactions such as diffusion appear to be rate limiting. It is not entirely clear that the mechanisms of time dependent crack growth are identical for different environment/alloy couples, or for different ranges of loading conditions. This paper will attempt to examine the chemical aspects of environment/alloy interactions and to correlate those aspects with observed crack propagation rates under a variety of loading conditions at or near room temperature. Additionally, a brief discussion of the role of environment on elevated temperature fatigue crack growth will be presented.			

14. KEY WORDS	LINK A		LINK B		LINK C	
	ROLE	WT	ROLE	WT	ROLE	WT
Crack Growth Stress Corrosion Cracking Corrosion Fatigue						

**THIS PAGE IS BEST QUALITY PRINTING FROM COPY FURNISHED TO DDC**

**INSTRUCTIONS**

1. **ORIGINATING ACTIVITY:** Enter the name and address of the contractor, subcontractor, grantee, Department of Defense activity or other organization (*corporate author*) issuing the report.
- 2a. **REPORT SECURITY CLASSIFICATION:** Enter the overall security classification of the report. Indicate whether "Restricted Data" is included. Marking is to be in accordance with appropriate security regulations.
- 2b. **GROUP:** Automatic downgrading is specified in DoD Directive 5200.10 and Armed Forces Industrial Manual. Enter the group number. Also, when applicable, show that optional markings have been used for Group 3 and Group 4 as authorized.
3. **REPORT TITLE:** Enter the complete report title in all capital letters. Titles in all cases should be unclassified. If a meaningful title cannot be selected without classification, show title classification in all capitals in parenthesis immediately following the title.
4. **DESCRIPTIVE NOTES:** If appropriate, enter the type of report, e.g., interim, progress, summary, annual, or final. Give the inclusive dates when a specific reporting period is covered.
5. **AUTHOR(S):** Enter the name(s) of author(s) as shown on or in the report. Enter last name, first name, middle initial. If military, show rank and branch of service. The name of the principal author is an absolute minimum requirement.
6. **REPORT DATE:** Enter the date of the report as day, month, year; or month, year. If more than one date appears on the report, use date of publication.
- 7a. **TOTAL NUMBER OF PAGES:** The total page count should follow normal pagination procedures, i.e., enter the number of pages containing information.
- 7b. **NUMBER OF REFERENCES:** Enter the total number of references cited in the report.
- 8a. **CONTRACT OR GRANT NUMBER:** If appropriate, enter the applicable number of the contract or grant under which the report was written.
- 8b, 8c, & 8d. **PROJECT NUMBER:** Enter the appropriate military department identification, such as project number, subproject number, system numbers, task number, etc.
- 9a. **ORIGINATOR'S REPORT NUMBER(S):** Enter the official report number by which the document will be identified and controlled by the originating activity. This number must be unique to this report.
- 9b. **OTHER REPORT NUMBER(S):** If the report has been assigned any other report numbers (*either by the originator or by the sponsor*), also enter this number(s).
10. **AVAILABILITY/LIMITATION NOTICES:** Enter any limitations on further dissemination of the report, other than those

imposed by security classification, using standard statements such as:

- (1) "Qualified requesters may obtain copies of this report from DDC."
- (2) "Foreign announcement and dissemination of this report by DDC is not authorized."
- (3) "U. S. Government agencies may obtain copies of this report directly from DDC. Other qualified DDC users shall request through \_\_\_\_\_."
- (4) "U. S. military agencies may obtain copies of this report directly from DDC. Other qualified users shall request through \_\_\_\_\_."
- (5) "All distribution of this report is controlled. Qualified DDC users shall request through \_\_\_\_\_."

If the report has been furnished to the Office of Technical Services, Department of Commerce, for sale to the public, indicate this fact and enter the price, if known.

11. **SUPPLEMENTARY NOTES:** Use for additional explanatory notes.

12. **SPONSORING MILITARY ACTIVITY:** Enter the name of the departmental project office or laboratory sponsoring (*paying for*) the research and development. Include address.

13. **ABSTRACT:** Enter an abstract giving a brief and factual summary of the document indicative of the report, even though it may also appear elsewhere in the body of the technical report. If additional space is required, a continuation sheet shall be attached.

It is highly desirable that the abstract of classified reports be unclassified. Each paragraph of the abstract shall end with an indication of the military security classification of the information in the paragraph, represented as (TS), (S), (C), or (U).

There is no limitation on the length of the abstract. However, the suggested length is from 150 to 225 words.

14. **KEY WORDS:** Key words are technically meaningful terms or short phrases that characterize a report and may be used as index entries for cataloging the report. Key words must be selected so that no security classification is required. Identifiers, such as equipment model designation, trade name, military project code name, geographic location, may be used as key words but will be followed by an indication of technical context. The assignment of links, roles, and weights is optional.